

Article

Optimization of the Storage Spaces and the Storing Route of the Pharmaceutical Logistics Robot

Ling Zhang ¹, Shiqing Lu ^{2,3,*}, Mulin Luo ² and Bin Dong ⁴

- ¹ Mechanical Engineering and Automation College, Chongqing Industry Polytechnic College, Yubei District, Chongqing 400050, China
- ² School of Mechanical Engineering, Chongqing University of Technology, Banan District, Chongqing 400045, China
- ³ Robot and Intelligent Manufacturing Technology, Key Laboratory of Chongqing Education Commission of China, Chongqing 400045, China
- ⁴ Chongqing Dile Jinchi General Machinery Co., Ltd., Chongqing 401320, China
- * Correspondence: shiqing.lu@cqut.edu.cn

Abstract: Auto drug distribution systems are used popularly to replace pharmacists when drugs are distributed in pharmacies. The Cartesian robot is usually used as the recovery mechanism. Under non-dynamic storage location conditions, generally, the selected planning route of the Cartesian robot is definite, which makes it difficult to optimize. In this paper, storage spaces were distributed for different drugs, and the route of storing was broken down into multiple path optimization problems for limited pick points. The path was chosen by an improved ant colony algorithm. Experiments showed that the algorithm can plan an effective storing route in the simulation and actual operation of the robot. The time spent on the route by improved ant colony algorithm sequence (IACS) was less than the time spent of route by random sequence (RS) and the time spent of route by traditional ant colony algorithm sequence (ACS); compared with RS, the optimized rate of restoring time with iacs can improve by 22.04% in simulation and 7.35% in operation. Compared with ACS, the optimized rate of restoring time with iacs was even more than 4.70% in simulation and 1.57% in operation. To the Cartesian robot, the optimization has certain guiding significance of the application on the 3D for improving quality.



Citation: Zhang, L.; Lu, S.; Luo, M.; Dong, B. Optimization of the Storage Spaces and the Storing Route of the Pharmaceutical Logistics Robot. *Actuators* **2023**, *12*, 133. <https://doi.org/10.3390/act12030133>

Academic Editor: Chih Jer Lin

Received: 13 February 2023

Revised: 16 March 2023

Accepted: 20 March 2023

Published: 21 March 2023



Copyright: © 2023 by the authors. Licensee MDPI, Basel, Switzerland. This article is an open access article distributed under the terms and conditions of the Creative Commons Attribution (CC BY) license (<https://creativecommons.org/licenses/by/4.0/>).

Keywords: Cartesian robot; storing route; ant colony algorithm

1. Introduction

As far as the safety of patients is concerned, the safety of the drugs distributed and managed is crucial. There are errors related to dispensing in the pharmacy every day. Dispensing errors, including drug shortages, account for 20–50% of all existing medication errors, and the dispensing error rate is 0.01–0.08% of drug distribution [1–4]. These are not only caused by subjective reasons, but also by objective reasons. For example, in many Asian countries, doctors must play a dual role between examining prescription drugs and dispensing drugs. Sometimes, the number of patients exceeds the capacity of most hospitals, which means that a large number of drugs need to be allocated [5]. Many dispensing devices and robots were developed to distribute and manage drugs in hospitals and pharmacies in order to reduce human errors, achieve a high response rate, and reduce labor intensity.

In the past three decades, the development of new technologies such as control technology, Internet technology, the Internet of Things, robots, artificial intelligence, and machine manufacturing promoted the development of drug recovery, distribution, and management, such as the Pharmacy Automation System (PAS). This was studied and used in many countries, including Germany, USA, Japan, China, and the Netherlands [6]. Between 1993 and 1997, the first fast medicine dispensing device, the Automatic Pharmacy

(AP), was designed, developed, and installed by the ROWA in Germany. It can be dispensed and recovered by the operator and electronic prescriptions can be issued automatically, rather than the manual work of pharmacists. The manipulator applied for an invention patent, but it has important shortcomings in terms of recovery efficiency [7]. Later, the drug dispensing system (DDS) was designed to rapidly dispense and recover drugs to meet the needs. With the use of DDS, errors were significantly improved; the errors were only dispensing errors, which is called a repeated error. In drug distribution [8,9], the dispensing error rate is not more than 0.03%. At the same time, a prescription takes 7 to 8 s, and DDS can save waiting time.

Under the normal operating conditions of the device, research fields such as recovering drugs, examining the names and quantities of drugs, and examining prescriptions were expanded. The difficulty and labor intensity of the operation were reduced. The recovery process is assisted by a manipulator. In this case, how to improve the working efficiency of the manipulator is actively studied.

The recovery process includes manually assisting the robot to replenish and restore drugs to the drug repository [10,11]. The recovery path is the planning path of the DDS medical logistics system, which is traditionally applied to the transportation system and warehouse storage of production and service departments [12]. Picking list is one of the main activities to be executed, which determines its operation cost and time [13,14]. Research shows that the proportion of order picking in the total operating cost of the warehouse is not less than 55–75% [15–17]. The drug warehouse is called “picking”, to distinguish it from the drug warehouse when selecting to store drugs. Therefore, an effective pickup and recovery route strategy is selected in FMDS to reduce costs, manpower, and time.

The storing strategy was a major task in previous works. The storing process was defined as a traveling salesman problem (TSP) or vehicle route problem (VRP) in the pharmaceutical logistics robot [18–20]. However, the storing process cannot simply be viewed as a customer in TSP or VRP because of the characteristics of the capacity of the manipulator and actual demand. The reason that one picking may be visited more than once is because a shortage of one picking may exceed the capacity of the manipulator. A novel storing strategy was proposed to store medicine in the logistics pharmaceutical robot. All picking points are assigned in multiple and different paths. The optimization problem we are now discussing is more about the point-to-point method, which is a vector problem [21]. In many cases, we only consider the point-to-point relationship, or more importantly, the optimization of the algorithm, or the increase or decrease in the intermediate constraints [22]. However, when applied in practical engineering, we found that driving by the motor will actually affect the in optimization of this path. Research this field is relatively few; at the same time, we also found that in rectangular coordinate robots, there will be differences in path caused optimization by different driving modes, and the impact of the motor drive is often not considered. For example, during the printing process, the driving of the motor of the 3D printer’s three-rectangular coordinate robot will indirectly affect the printing [23]. Therefore, different ways of the same drive will have different effects on the optimization of this path.

At present, domestic and foreign researchers made many achievements in the research of storage allocation. J. Giacomo Lanza et al. [24] proposed a mixed integer linear programming (MILP) model based on multi-commodity flow formula, which had some effective inequalities. Two relaxation methods were also proposed to estimate the quality of the model solution. Then, two mathematical methods were designed from the MILP model. Xiangbin Xu et al. [25] proposed a distributed storage location allocation (MPSSLA) strategy based on multiple sorters, which can achieve better optimization effect than the traditional centralized storage strategy in the multi-picker to parts picking system. Zhong Qiang Ma et al. [26] proposed a heuristic algorithm to select the minimum number of shelves and evaluate the optimization effect of SA-VNSSA and SCSPCC on the number of shelves transferred. At the same time, intelligent algorithms such as particle swarm optimization

(PSO), genetic algorithm (GA), and ant colony optimization (ACO) were used to optimize the storage path of the drug logistics robot [27,28]. In terms of searching optimized storage paths, PSO proposed by James Kennedy, GA [29] proposed by John Holland, and ACO proposed by Marco Dorigo can effectively reduce the number of values or manipulators of different storage paths to achieve the purpose of optimization. Because there are few adjustable parameters, the structure of PSO is simple, but more iterations are needed to obtain the best result of problem solving. For GA, the number of ants and the number of picking points 5 and 15 are close to or the same, and ACO is better than GA in searching TSP optimization solution [30].

All picking points may be assigned in multiple and different paths, and all paths form the route that is stored. The route is regarded as a multiple of TSP, and the order of drug stored is optimized in each TSP. The remainder of this paper is structured as follows. In Section 2, the structure of storage and storing manipulator are described. Storing models and optimized algorithms are shown in Section 3. Simulation, operations, and experimental analysis are conducted in Section 4. Finally, the conclusion and future work are provided in Section 5.

2. Storage Unit Structure

2.1. Description of the Storage

The structure of the medicine storage and distribution equipment proposed in this paper includes two parts: a medicine-grabbing manipulator and a slope-type medicine storage tank, as shown in Figure 1. The medicine-grabbing manipulator is mainly used to provide real-time supply of drugs, ensure sufficient inventory of drugs in the automated pharmacy, and meet the demand for dispensing drugs in the pharmacy. The slope-type drug storage tank is responsible for storing and managing a certain number of regular boxed drugs, maximizing the drug storage within the effective storage area, ensuring drug supply during peak periods of drug delivery, and facilitating connection with the dispensing and dispensing systems.

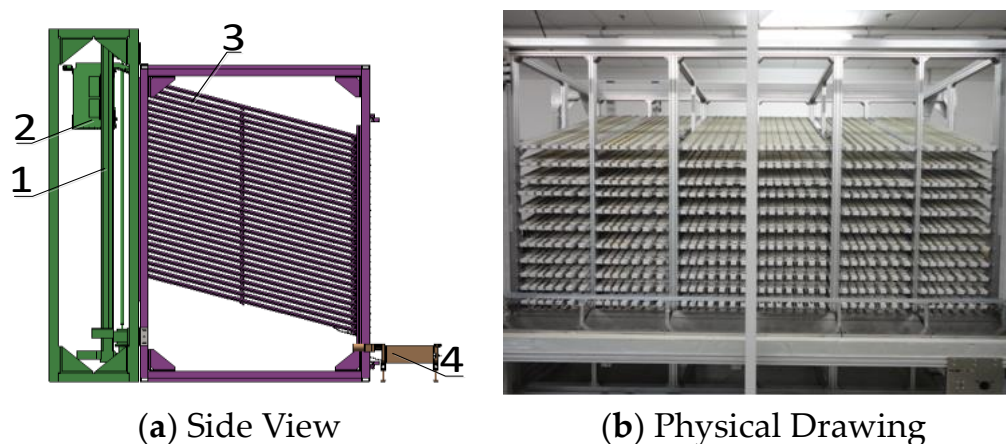


Figure 1. 3D and physical picture of the medicine storage system. 1. Cartesian coordinate robot. 2. Dispensing manipulator 3. Sloping drug storage 4. Automatic drug delivery device.

In this paper, the U-shaped storage structure of the roller and the direct-acting tilting plate type drug delivery mechanism were used. The U-shaped storage position of roller is mainly composed of a roller, roller shaft, spacer bar, frame, and beam. Generally, a nylon roller with a diameter of 10 mm is used to cover the roller shaft and evenly distributed at a spacing of 20 mm. When the roller is installed to a certain number, the spacer bar will be added. The two adjacent spacer bars form the smallest storage unit, called storage position. Several storage positions form a drug storage tank, as shown in Figure 2. Since the principle of gravity dropping is adopted, there needs to be an angle between the medicine storage tank and the horizontal plane to ensure the medicine and the size of the angle will affect

the installation quantity of the medicine storage tank. Therefore, it is necessary to calculate the inclination angle of the medicine storage tank and the friction coefficient of nylon and paper $f_1 = 0.3\text{--}0.4$.

$$G \sin \alpha = \mu G \cos \alpha \tag{1}$$

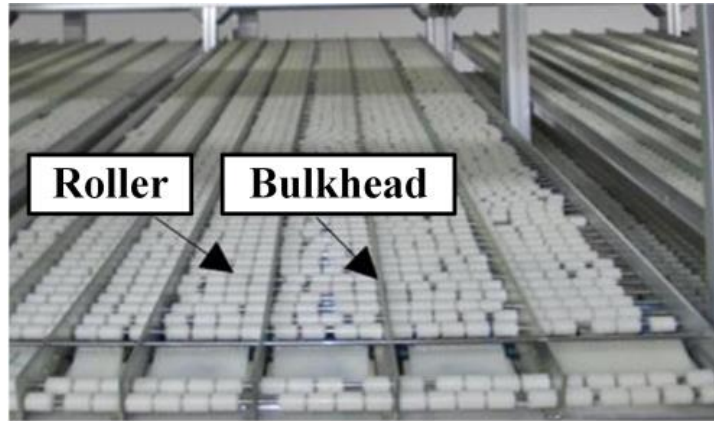


Figure 2. U-shaped storage position and medicine storage tank.

Figure 3 shows the side view of the storage tank. From this, it can obtain the α angle range, $\alpha_1 = 16.99^\circ$, $\alpha_2 = 21.8^\circ$. Due to air resistance, the best angle was finally set at 18° . The number of medical tanks will be reduced when the angle of the tank becomes larger, but this is beneficial for the downward movement of the medical tank. The total thickness of the frame and partition of the medicine storage tank was 32 mm, and the spacing between two adjacent drug storage tanks was 40 mm. The outer frame size of the rapid dispensing system was 3540 mm \times 1440 mm \times 2450 mm, and the size of its drug storage mechanism was $l_1 = 1260$ mm, $h = 2050$ mm.

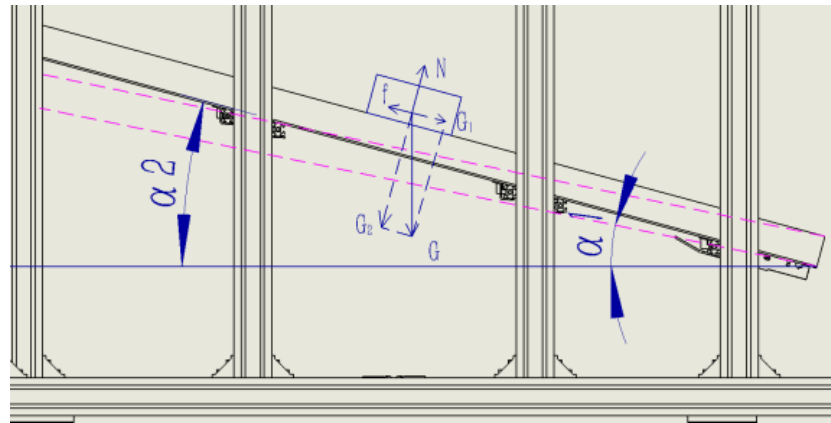


Figure 3. Side view of medicine storage tank.

According to the side diagram of the storage slot in Figure 4, the number of layers in the tank m was calculated:

$$m = \frac{h - l_1 \tan \beta}{h_2 / \cos \beta} = \frac{(h - l_1 \tan \beta) \cos \beta}{h_2} \tag{2}$$

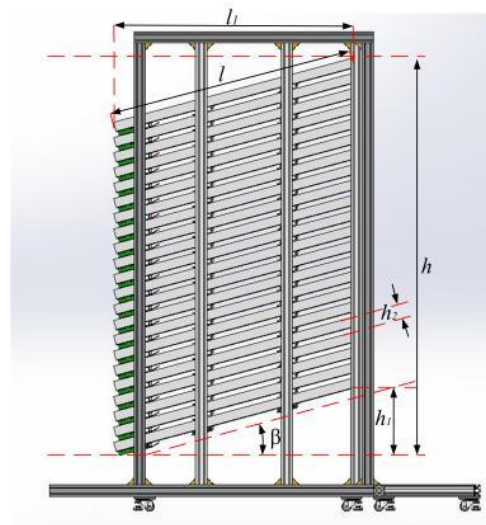


Figure 4. Side view of drug storage tank.

The results are shown in Table 1. It can be observed that the number of layers that can be stored in the storage tank varied with different angles. When the tilt angle was 18° , the space utilization rate was 10% higher than that with 21.8° . It can be observed that the use of 18° roller U-shaped storage tank was in line with the optimal distribution.

Table 1. Quantity of medicine storage tanks with different tilt angles.

β	h_1 (m)	h_2 (m)	m
18°	0.4095	1.640	20
20°	0.4586	1.591	19
21.8°	0.5040	1.546	18

The direct-acting flap type drug delivery mechanism is linked to the lifting baffle via the slider mechanism, and the movement of the lifting baffle is realized by pulling the slider through the electromagnet. The advantage of this drug delivery method is that the drug delivery mechanism will not hit the drug box during the drug delivery process. Therefore, the downward angle of the drug will not change and will not reverse. At the same time, it will also reduce the situation that a small number of drugs cannot be delivered due to the reduction in the delivery angle of the drug box.

For the direct-acting flap type drug delivery mechanism, the experimental results are shown in Tables 2 and 3, where the baffle height was 5 mm. The test equipment is shown in Figures 5 and 6.

Table 2. Delivery time of test drugs (test kit size: $130 \text{ mm} \times 95 \text{ mm} \times 12 \text{ mm}$).

Number of Remaining Medicine Boxes in the Medicine Storage Tank	7	6	5	4	3	2	1
Single Box Dispensing Time	0.311	0.328	0.335	0.334	0.369	0.392	0.468

Table 3. Outgoing test results of different kits.

Kit Size (mm)	Delivery Time (s)	No Drug Delivery
$167 \times 67 \times 17$	0.655	Two boxes and above
$130 \times 95 \times 12$	0.362	nothing
$98 \times 47 \times 12$	0.377	One box



Figure 5. Simple drug delivery mechanism.



Figure 6. Experimental diagram.

It was observed in the above experiments that the control of the drug delivery time of the flap type drug delivery mechanism was not different, but when the drug was light, the gravity was not enough to overcome the friction, and the drug box would not slide. At the same time, when the medicine was heavy and the quantity in the medicine storage tank was too large, the first box of medicine was squeezed by the medicine behind, and when the electromagnetic force was small, it was not able to leave the warehouse. To sum up, the flap type drug delivery mechanism has a fast delivery speed and can meet the requirements of drug delivery in any situation.

To ensure the uniqueness of drug storage and distribution in each unit, the following settings were established:

- (1) The drug storage and distribution system is a rectangular frame structure, as shown in Figure 3. The drug storage and distribution system is composed of six storage units, each of which is composed of multi-layer drug storage tanks, and each of which is composed of multiple storage locations;

- (2) The length of each tank is the same, but the width and height are different. The storage height of the same layer is the same. After the equipment runs, each storage location can only store a certain drug;
- (3) Set the drug storage and distribution system to be composed of M drug storage tanks. Since the width of drugs that can be stored in each unit is limited when setting, the storage unit needs to be optimized first;
- (4) Set the drug r to be stored for the first time, the drug width is l_r , where the inventory of the drug storage tank is $s = 0$, and the length of the drug storage tank is L , and then, the number of replenishment required for the drug storage tank is $s_r = \lceil L/l_r \rceil$;
- (5) For the storage of a certain drug, the number of storage units allocated is N . Since the length of storage units is the same, the number of this drug stored in each unit is the same;
- (6) It is set that there are n rows of m layers in the reservoir rectangle, and the reservoirs in row j of layer i are recorded as (i, j) , where $i = 1, 2, \dots, m; j = 1, 2, \dots, n$;
- (7) Each chemical storage tank has a unique number, among which, the storage location number in column j of layer i is $ID_{ij} = 100 \times i + j$, and the chemical storage tank code is arranged from small to large. If a chemical storage tank has been allocated, the corresponding mark is 1, otherwise it is idle, and the mark is 0.

2.2. Description of the Sorting Mechanical Configuration and Sorting Process

The principle of the end effector is similar to that of the striker ejection, and so, it is referred to as the clip manipulator (as shown in Figure 7). Before medicine replenishment, the medicine is stored in the tray (similar to a cartridge). Because the height of each medicine box is different, the maximum number of medicine boxes stored in the tray also varies. The number of medicine boxes that can be stored in the tray is controlled and managed by the software system.



Figure 7. End actuator. 1.Chain clamping device. 2. Flexible tensioning device. 3. Detection sensor. 4. Motor.

In order to ensure the accuracy and stability of the end effector desired position during the process of medicine supplement, the form of rectangular coordinate robot is adopted in the design. The robot is composed of two groups of linear motion units. The end actuator is installed on two vertical linear motion units in the X direction and connected to the Y-axis guide rail through a slider. The end actuator and X-axis guide rail have a certain tilt angle. The movement in the Y direction is connected by the synchronous axis, and the motor drives the synchronous axis movement, which can realize the movement of the end actuator and the X-axis guide rail in the Y direction, that is, the horizontal movement of the end actuator. The movement in the X direction is directly driven by the motor to realize the movement of the end actuator on the X-axis guide rail, that is, the vertical movement of the end actuator, as shown in Figure 8.

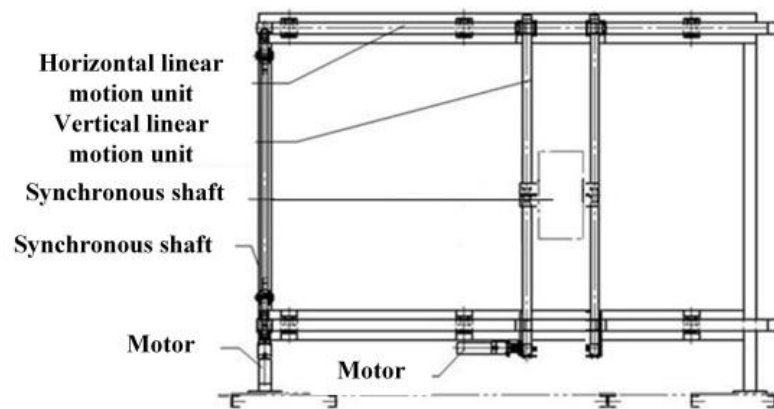


Figure 8. X-Y rectangular coordinate robot.

In the storage of certain drugs, a different number of drug storage tanks will be allocated according to their distribution frequency. Although there are many drug storage tanks, there are not many drug storage tanks for a certain drug for hundreds of drug storage types. In general, the quantity of a drug placed into the equipment shall be as much as possible to ensure its half day distribution. The resulting drugs need to be quickly replenished at any time. Generally, the pharmacy will set the times of replenishment within a day according to the drug consumption, but at the same time, if a drug is less than $1/4$ of the total storage of the drug, the system will also remind the temporary replenishment.

The process of restoring (replenishment drug process) is somewhat similar to the traveling salesman problem (TSP), but it is not completely the same. Due to the limited capacity of the manipulator, the quantity of replenishment at one time is limited, and the inventory quantity of the drug storage tank is generally greater than the capacity of the manipulator. Therefore, in general, the manipulator will replenish a certain drug storage tank according to the maximum capacity. When the shortage of the drug storage tank is less than the manipulator's capacity, it will be considered to complete the replenishment together with other drug storage tanks. Therefore, for a certain drug, its replenishment process includes all the drug storage tanks storing the drug, while for the drug storage tank, its replenishment process is divided into two parts: point-to-point replenishment and mixed replenishment.

3. Optimization of Sorting Route

3.1. Amount of Storing with a Kind Drug

The storage route of drugs includes the path of point-to-point replenishment and the mixed replenishment path. Before calculating its path, it is necessary to determine the replenishment time of the point-to-point replenishment process and the points of each replenishment during the mixed replenishment path.

First of all, the point-to-point time of shortage in each drug storage tank are separated. The specific separation model is as follows:

$$\begin{cases} s_{ij}^r = \lfloor L/l_r \rfloor \\ s_{ij}^{r1} = \lfloor s_{ij}^r / Q \rfloor \\ s_{ij}^{r2} = s_{ij}^r - s_{ij}^{r1} Q \end{cases} \quad (3)$$

where Q is the maximum quantity of medicine r that can be carried by the manipulator, s_{ij}^r is the maximum quantity of medicine r stored in the ij medicine storage tank, s_{ij}^{r1} is the number of point-to-point replenishment of medicine r stored in the medicine storage tank, and s_{ij}^{r2} is the quantity of out-of-stock of point-to-point replenishment removed by the medicine storage tank.

The number of point-to-point supplements s_r^1 is,

$$s_r^1 = \sum_{a=1}^N s_{ij}^{r1} \tag{4}$$

In the Formula, the drug r is assigned N drug storage tanks, where $a = 1, 2, \dots, N$. The number of mixed replenishment s_r^2 is,

$$s_r^2 = \begin{cases} s_r^2 & \sum_{a=1}^N s_{ij}^{r2} < Q \\ s_r^2 + 1 & \sum_{a=1}^N s_{ij}^{r2} \leq Q, \sum_{b=a+1}^N s_{ij}^{r2} > Q \end{cases} \tag{5}$$

3.2. Design of the Ant Colony Algorithm

The ant colony algorithm (AC) is a heuristic algorithm used to simulate the behavior of real ant colony when establishing the shortest path between a food source and nest. When an ant moves, it releases a trace pheromone that can be detected by other ants. As more ants pass through the path, more pheromones are deposited. Because ants move according to the number of pheromones, the richer the pheromone tracks on the path, the greater the possibility of other ants tracking it. Therefore, ants can build the shortest path from the nest to the food source and return.

In the supplement process, whether it is point-to-point supplement or mixed supplement, its supplement path is composed of all paths from the previous supplement point (including the initial point) to the next supplement point. Set the previous supplement point of drug r as the (i, j) drug storage tank, and the next supplement point as the $(i + e, j + f)$ drug storage tank. e, f are arbitrary rational numbers. A unit of X coordinate or Y coordinate denotes that length is different in each drug storage; to simplify our modeling, the value is set to 12 cm. The corresponding supplementary distance is,

$$\begin{cases} l_{(i, i+e),(j,j+f)}^{rx} = 0.12e \\ l_{(i, i+e),(j,j+f)}^{ry} = 0.12f \end{cases} \tag{6}$$

The time it takes from (i, j) to $(i + e, j + f)$ on the X and Y axes is,

$$t_{(i, i+e),(j,j+f)}^{rx} = \begin{cases} 2\sqrt{\frac{l_{(i, i+e),(j,j+f)}^{rx}}{a_x}} & \text{if } \frac{v_x}{a_x} > \sqrt{\frac{2l_{(i, i+e),(j,j+f)}^{rx}}{a_x}} \\ 2\left(\frac{v_x}{a_x} + \sqrt{\frac{l_{(i, i+e),(j,j+f)}^{rx} - v_x/a_x}{a_x}}\right) & \text{other} \end{cases} \tag{7}$$

$$t_{(i, i+e),(j,j+f)}^{ry} = \begin{cases} 2\sqrt{\frac{l_{(i, i+e),(j,j+f)}^{ry}}{a_y}} & \text{if } \frac{v_y}{a_y} > \sqrt{\frac{2l_{(i, i+e),(j,j+f)}^{ry}}{a_y}} \\ 2\left(\frac{v_y}{a_y} + \sqrt{\frac{l_{(i, i+e),(j,j+f)}^{ry} - v_y/a_y}{a_y}}\right) & \text{other} \end{cases} \tag{8}$$

Pickings must be defined on a graph as $G = \{V, E\}$, where $V = \{0\} \cup N$ is the vertex set and E is the arc set.

Pheromone concentration is defined as $\tau_{ij}(t)$ at t moment on the edge between picking i and picking j . It is equal to $\Delta\tau_{ij}(t) = 0, t = 0$. Over time, the pheromone concentration on the path is changed because of new pheromone being applied and old pheromone evaporating. ρ is set as volatility coefficient of the pheromone and showed the speed of evaporation. When all ants completed one tour, the pheromone on each path is given as:

$$\tau_{ij}(t+1) = (1 - \rho)\tau_{ij}(t) + \Delta\tau_{ij}(t) \tag{9}$$

where $\Delta\tau_{ij}(t) = \sum_{k=1}^m \Delta\tau_{ij}^k(t)$.

The pheromone concentration is defined as $\Delta\tau_{ij}^k(t)$, and it is released on the path from picking i to picking j by ant k . The pheromone value is determined with the ant's performance. A shorter path meant more pheromone is applied by the unit. Ant-cycle was used in this paper.

$$\Delta\tau_{ij}^k(t, t+1) = \begin{cases} Q/L_k & \text{the path from picking } i \text{ to picking } j \text{ by the ant } k \\ 0 & \text{other} \end{cases} \quad (10)$$

where Q is a constant, and L_k is the length of the tour constructed by ant k .

$$P_{ij}^k = \begin{cases} \frac{\tau_{ij}^\alpha \eta_{ij}^\beta}{\sum_{j \in allowed_k} \tau_{ij}^\alpha \eta_{ij}^\beta} & \text{if } j \in allowed_k \\ 0 & \text{other} \end{cases} \quad (11)$$

$$\eta_{ij}(t) = 1/d_{ij} \quad (12)$$

where P_{ij}^k is the selection probability.

$allowed_k = (v_1, v_2, \dots, v_n) - tabU_k$ represents the collection of locations that could be chosen by ant k . $tabU_k (k = 1, 2, \dots, m)$ is the taboo list of ant k . The visited location is recorded in the taboo list, and the memory of ant k is illustrated. The inverse distance between picking i and picking j is shown as $\eta_{ij}(t)$, which is the visibility of moving from city i to city j . α is the residual degree of information on (i, j) edge. β is the heuristic degree of information. Both of them could be changed by the user.

A new d_{ij} can be obtained from Formulas (6)–(8),

$$d_{ij} = \begin{cases} l_{(i, i+e), (j, j+f)}^{rx} & t_{(i, i+e), (j, j+f)}^{rx} \geq t_{(i, i+e), (j, j+f)}^{ry} \\ l_{(i, i+e), (j, j+f)}^{ry} & \text{other} \end{cases} \quad (13)$$

Meanwhile, the L'_k is calculated by Formula (13),

$$L'_k = \sum_{i=0}^{j=N} d'_{ij} \quad (14)$$

where L'_k is the time of the tour constructed by ant k .

It can be obtained from Formula (14),

$$\Delta\tau_{ij}^k(t, t+1) = \begin{cases} Q/L'_k & \text{the path from picking } i \text{ to picking } j \text{ by the ant } k \\ 0 & \text{other} \end{cases} \quad (15)$$

Combining Equations (11), (12) and (15), the new transfer possibility, P_{ij}^k , between picking i and picking j are calculated.

3.3. The Process of the Algorithm

Based on Section 3.2, the actual pseudocode of the improved ant colony algorithm is as follows (Algorithm 1):

Algorithm 1. (improved ant colony algorithm sequence (iacs))

Initialize $\alpha, \beta, \tau_0, \rho, Q, n, Nc_max, S_x, S_y, V_x, V_y, a_x, a_y$
While ($nc \leq Nc_max$)
 Initialize refilling time $T_k, tabU_k$, and $allowed_k$
 For ($k=1; k < m; k++$)
 While ($allowed_k \neq null$)
 Build $tabU_k$ by applying $n-1$ times the following step
 $tabU_k = tabU_k + (i, j)$ and $allowed_k = allowed_k - (i, j)$
 Choose the next node j probability, calculate P_{ij}^k according to the Formula (11):

$$P_{ij}^k = \begin{cases} \frac{\tau_{ij}^\alpha \eta_{ij}^\beta}{\sum_{j \in allowed_k} \tau_{ij}^\alpha \eta_{ij}^\beta} & \text{if } j \in allowed_k \\ 0 & \text{other} \end{cases}$$
 Calculate the optimal tour L_k of ant k
 End while
 For every edge (i, j)
 Update the pheromone according to the Formulas (9) and (12):
 $\tau_{ij}(t+1) = (1 - \rho)\tau_{ij}(t) + \Delta\tau_{ij}(t)$
 $\Delta\tau_{ij}(t)$ by applying the rule:

$$\Delta\tau_{ij}(t) = \sum_{k=1}^m \Delta\tau_{ij}^k(t)$$
 where $\Delta\tau_{ij}^k$ is the same as Equation (15):

$$\Delta\tau_{ij}^k(t) = \frac{Q}{L_k}$$
 End for
 End for
 Update the historical optimal storing path d_{ij}
 where d_{ij} is updated as Equation (13)
 For every edge (i, j) do
 $\tau_{ij} = (nc+1)\tau_{ij}(nc)$
 End For
End while

4. Experiments and Analysis

4.1. Test Samples

Some experiments were conducted to test the quality of searching restoring route to different selection methods by the random sequence (rs), the traditional ant colony algorithm sequence (acs), and the improved ant colony algorithm sequence (iacs). Test samples, two kinds of medicine, are described as follows. The width of an ordinary medicine box was in the range of 35–110 mm and the height was in the range of 10–60 mm. The test samples are shown in Table 4.

Table 4. Medicine information of test samples.

Number	Medicine Name	Pharmaceutical Manufacturers	H (mm)	Max
1	Ritodrine Hydrochloride Tablets	Biotech, Ltd. TAIWAN	10.85	30
2	Polyferose Capsules	Qingdao Guofeng Pharmaceutical Co., Ltd.	15.90	20

The test category included 5, 10, 15, and 20 selections. As shown in Table 5, the test categories of two test samples are listed. SPP indicates a picking shortage, and ORT indicates picking order according to storage time. For example, 101 in the table represents the first of the first layer in the drug storage equipment. In the first test sample, the number of SPPs was balanced, so the robot had five pick points for each drug recovery. In the second test sample, the number of SPPs was different, and so, the picking points of the robot for each drug for recovery were changed from 8 to 2.

Table 5. Shortage and order of test samples.

Number	Picking	101	103	109	202	208	211	212	303	305	307
1	ORT	11	5	19	17	6	3	18	10	14	20
	SPP	6	3	4	5	7	5	2	7	7	10
	Picking	408	409	502	507	512	601	608	707	709	711
	ORT	16	15	8	4	12	7	13	2	9	1
	SPP	4	6	3	8	4	4	5	8	7	3
	Number	Picking	103	104	107	201	207	202	210	302	305
2	ORT	19	1	4	16	20	14	3	8	2	13
	SPP	5	4	2	6	5	1	2	1	4	6
	Picking	409	403	404	509	108	602	606	611	706	707
	ORT	10	7	12	18	17	6	11	15	5	9
	SPP	4	3	1	10	3	3	2	2	1	3

4.2. Results and Analysis of Test Samples

The simulation experimental data of the test samples are expressed in Table 6.

Table 6. Simulation results of different storing models.

Number	Storing Model	Route	Storing Route Value (m)	Route Rate	Storing Time (s)	Time Rate
a1-1	rs	0-103-507-211-707-711-0	3.7261	0	11.3895	0
b1-1	acs	0-103-211-711-707-507-0	3.0827	17.26%	10.3353	9.26%
c1-1	iacs	0-103-507-707-211-711-0	3.5261	5.37%	10.1490	10.89%
a1-2	rs	0-208-601-502-709-303-0	7.3718	0	22.8189	0
b1-2	acs	0-303-208-709-502-601-0	6.0045	18.55%	19.7200	13.58%
c1-2	iacs	0-208-709-601-502-303-0	6.4561	12.42%	19.2517	15.63%
a1-3	rs	0-512-608-305-409-101-0	10.9175	0	33.9041	0
b1-3	acs	0-305-409-512-608-101-0	8.7301	20.03%	29.6905	12.43%
c1-3	iacs	0-512-409-608-305-101-0	9.3088	14.74%	28.3970	16.24%
a1-4	rs	0-408-202-212-109-307-0	14.8050	0	45.9859	0
b1-4	acs	0-109-212-408-307-202-0	11.3332	23.45%	39.0516	15.08%
c1-4	iacs	0-212-109-307-408-202-0	12.1811	17.72%	37.3981	18.67%
a2-1	rs	0-104-305-210-107-706-602-403-302-0	3.2082	0	12.0624	0
b2-1	acs	0-104-305-107-210-706-602-403-302-0	3.0132	6.08%	11.1822	7.30%
c2-1	iacs	0-302-104-305-107-210-706-403-602-0	3.3867	-5.56%	10.8914	9.71%
a2-2	rs	0-611-202-301-404-707-409-606-0	7.8976	0	25.3772	0
b2-2	acs	0-202-309-611-707-606-404-301-0	5.7759	26.87%	20.9768	17.34%
c2-2	iacs	0-611-409-707-606-404-202-301-0	6.4479	18.36%	19.7844	22.04%
a2-3	rs	0-108-509-207-0	10.2047	0	32.5624	0
b2-3	acs	0-108-207-509-0	8.1137	20.49%	27.8004	14.62%
c2-3	iacs	0-108-207-509-0	8.7857	13.91%	26.6080	18.29%
a2-4	rs	0-103-204-0	11.1096	0	36.4167	0
b2-4	acs	0-103-204-0	9.0186	18.82%	31.6547	13.08%
c2-4	iacs	0-103-204-0	9.6906	12.77%	30.4623	16.35%

The comparison can be summarized as follows.

- (1) In the first test sample, compare the recovery paths between the three models. They were completely different from other models. The recovery path includes all recovery paths in the storage process of a drug. The recovery path lengths of rs, acs, and iacs were 14.8050, 11.3332, and 12.1811, respectively. Based on this, we can see that the recovery path of acs was the shortest. Compared with rs, the best recovery path rate

of acs and iacs was more than 23.45% and 17.72%, respectively. It can be seen that the optimized rate between the acs and the iacs based on the rs was more than 5.37%. Moreover, restoring time of the acs and the iacs were the difference. Both of them required shorter time than the rs on restoring route. The optimized rate of restoring time of both the acs and the iacs were shorter than 15.08% and 18.67% when compared with that of the rs. It can be seen that the acs can search shorter sorting routes than the rs and the iacs. In terms of storing time, the iacs was better than the rs and the acs. Accordingly, the objective function of the iacs was to achieve the shortest sorting time, and the objective function of the acs was to search the shortest storing route.

- (2) In the second test sample, comparing restoring paths among the three models, the rs were different from the acs and the iacs. Only one storing route was same as the acs and the iacs in four storing paths. Because it included two picking points which only has kind of storing route. it could not be optimized. The lengths of storing route of the rs, the acs, and the iacs were 11.1096, 9.0186, and 9.6906, respectively. Therefore, the acs is the best storing model to search the shortest storing route. The results showed that when the storage path of rs was properly arranged, the storage path of iacs was longer than that of rs. However, this rarely happens. However, iacs was better than rs and ac in terms of storage time. Compared with rs and acs, the optimal storage time of iacs was 16.35% and 3.27% shorter, respectively. It can be seen that iacs was the best storage model for searching storage paths and needed the shortest time.
- (3) In Table 6, as the number of pickings increased, the optimized rate on the storing route value and storing time also increased. The iacs was obviously shorter than the acs on storing time.

The operation experimental data of the test samples are expressed in Table 7.

Table 7. Operation test results of different storing models.

Number	Storing Model	Operation Time (s)	Storing Route Time (s)	Operation Rate	Storing Rate
a1-1	rs	46.490	11.390	0	0
b1-1	acs	45.435	10.335	2.32%	9.26%
c1-1	iacs	45.249	10.149	2.67%	10.89%
a1-2	rs	94.319	22.819	0	0
b1-2	acs	91.220	19.720	3.29%	13.58%
c1-2	iacs	90.752	19.252	3.78%	15.63%
a1-3	rs	141.804	33.904	0	0
b1-3	acs	137.591	29.691	2.97%	12.43%
c1-3	iacs	136.297	28.397	3.88%	16.24%
a1-4	rs	186.386	45.986	0	0
b1-4	acs	179.452	39.052	3.72%	15.08%
c1-4	iacs	177.798	37.398	4.61%	18.67%
a2-1	rs	38.062	12.062	0	0
b2-1	acs	37.182	11.182	2.31%	7.30%
c2-1	iacs	36.891	10.891	3.08%	9.71%
a2-2	rs	76.077	25.377	0	0
b2-2	acs	71.677	20.977	5.78%	17.34%
c2-2	iacs	70.484	19.784	7.35%	22.04%
a2-3	rs	107.962	32.562	0	0
b2-3	acs	103.200	27.800	4.41%	14.62%
c2-3	iacs	102.008	26.608	5.51%	18.29%
a2-4	rs	124.817	36.417	0	0
b2-4	acs	120.055	31.655	3.82%	13.08%
c2-4	iacs	118.862	30.462	4.77%	16.35%

The comparison can be summarized as follows.

- (1) In Table 7, comparing with the operation time or storing route time of the first test sample, the iacs was better than the rs and the acs. The optimized rate of operation time was more than 4.61% when comparing the iacs with the rs. Additionally, the optimized rate of operation time was more than 18.67% when comparing the iacs with the rs. The reason for this is that the storage time included in the operation time was not optimized. Optimization of the acs and the iacs were negative to the storing route. It can be seen that the iacs was better than the acs. The reason for this is that acceleration and deceleration of motor were set as “S” curve in actual operation and were set as oblique straight line in the simulation. The storing route of the iacs was longer than the acs’s in the first test sample. However, the iacs required less time to operate through this storing path than the acs. Additionally, the time used in operation, which was spent on storing path, was less than that used in the simulation when the storing path was short.
- (2) In Table 7, comparing with the operation time and storing route time of the second test sample, the iacs was also better than the rs and the acs. The optimized rate of operation time was more than 4.77% when comparing the iacs with the rs. The optimized rate of operation time was more than 16.35% when comparing the iacs with the rs. It can be seen that the optimized effect was similar to the first test sample. The optimization of the iacs was better than the acs. Compared with the rs, optimized rate of operation storing time with the iacs and the acs were both reducing instead. The reason for this is that with the increase in selection, more rs storage time was required, which was set as the denominator and had a greater impact.
- (3) In conclusion, the iacs was better than the rs on storing time. As picking increased, the iacs was obviously better than the acs. Based on the storing time of the rs, compared with the acs, the optimized rate of storing time with the iacs was more than 0.35%, even up to 1.57%.

5. Conclusions

This paper first increased the maximum storage capacity of the device by optimizing the storage space of the drug storage device, and then, optimized the main path of the device. It not only improved the effective use of the space of the device, but also enhanced the efficiency of drug delivery by the device.

Through the research on the inclination of the storage tank, 18° was selected to meet the minimum angle used. Therefore, under the condition of ensuring the smooth delivery of the drug delivery equipment and the largest number of storage, the storage space of the equipment was optimized, and the optimization result was 10% higher than the space of the most conventional angle (21.8°).

Based on this space, a multiple local TSP model based on improved ant colony optimization was proposed to increase storing efficiency and consider the acceleration and deceleration of the motor during actual storing process. Compared with the rs, both of the acs and the iacs were better on searching storing route and the storing time of the storing route was shorter. Compared with the rs, the optimized rate of storing route with the acs was more than 3.72% in actual operation. Compared with the rs, the optimized rate of storing route with the iacs was more than 4.61% in actual operation. Additionally, therefore, the iacs is a suitable storing model in the pharmaceutical logistics robot. Meanwhile, it was observed that storing time of the iacs was shorter than that of the acs. Moreover, it was more evident when the pickings increased. Based on the storing time of the rs, compared with the acs, the optimized rate of storing time with the iacs was more than 0.35%, even up to 1.57%. So, acceleration and deceleration were considered in the model, which is necessary.

Author Contributions: Conceptualization, L.Z. and M.L.; methodology, M.L. and B.D.; validation, L.Z., S.L. and M.L.; resources, L.Z. and S.L.; experiment, M.L.; writing, L.Z., M.L. and B.D.; funding acquisition, L.Z. All authors have read and agreed to the published version of the manuscript.

Funding: This research was funded by the Science and Technology Research Program of Chongqing Education Commission of China (KJQN202003202, KJQN202001127).

Data Availability Statement: The research simulation and experimental data of our paper are reflected in the pictures and tables in the manuscript. Therefore, no new dataset link was established.

Acknowledgments: We thank Hu for his suggestions on revising the English style of this paper.

Conflicts of Interest: The authors declare that there are no conflict of interest regarding the publication of this paper.

References

1. Tan, L.; Chen, W.; He, B.; Zhu, J.; Cen, X.; Feng, H. A survey of prescription errors in paediatric outpatients in multi-primary care settings: The implementation of an electronic pre-prescription system. *Front. Pediatr.* **2022**, *10*. [[CrossRef](#)] [[PubMed](#)]
2. Anjalee, J.A.L.; Rutter, V.; Samaranyake, N.R. Application of failure mode and effects analysis (FMEA) to improve medication safety in the dispensing process—A study at a teaching hospital, Sri Lanka. *BMC Public Health* **2021**, *21*, 1430. [[CrossRef](#)]
3. Nermeen, A.; Safa, A.; Sayed, S.; Mojeba, H. Studying the medication prescribing errors in the Egyptian community pharmacies. *Asian J. Pharm.* **2018**, *12*, 25–30.
4. Hesse, M.; Thylstrup, B.; Seid, A.K.; Tjagvad, C.; Clausen, T. A retrospective cohort study of medication dispensing at pharmacies: Administration matters! *Drug Alcohol Depend.* **2021**, *225*, 108792. [[CrossRef](#)] [[PubMed](#)]
5. Jacobson, M.G.; Chang, T.Y.; Earle, C.C.; Newhouse, J.P. Physician agency and patient survival. *J. Econ. Behav. Organ.* **2017**, *134*, 27–47. [[CrossRef](#)]
6. Chen, F.Y. Current situation and new progress of automated pharmacy. *Mingyi Dr.* **2020**, *4*, 277.
7. Cai, Y.X.; Zhang, M.L. Study on dispensing optimization of integrated traditional Chinese medicine dispensing system. *Light Ind. Mach.* **2019**, *37*, 80–88.
8. Jin, H.; Yun, C.; Wang, W.; Li, D.J. Application and research of the Clip Type Manipulator. In *Mechanisms and Machine Science*; Springer: Cham, Switzerland, 2016; pp. 841–851. [[CrossRef](#)]
9. Lin, Y.; Cai, Z.; Huang, M.; Gao, X.; Yu, G. Evaluation of development status and application effect of outpatient pharmacy automatic dispensing system in mainland China. *Chin. J. Mod. Appl. Pharm.* **2020**, *37*, 1131–1138.
10. Ozden, S.G.; Smith, A.E.; Gue, K.R. A computational software system to design order picking warehouses. *Comput. Oper. Res.* **2021**, *132*, 105311. [[CrossRef](#)]
11. Mulac, A.; Mathiesen, L.; Taxis, K.; Granås, A.G. Barcode medication administration technology use in hospital practice: A mixed-methods observational study of policy deviations. *BMJ Qual. Saf.* **2021**, *30*, 1021–1030. [[CrossRef](#)]
12. Jin, H.; He, Q.; He, M.; Lu, S.; Hu, F.; Hao, D. Optimization for medical logistics robot based on model of traveling salesman problems and vehicle routing problems. *Int. J. Adv. Robot. Syst.* **2021**, *18*, 17298814211022539. [[CrossRef](#)]
13. Sng, Y.L.; Ong, C.K.; Lai, Y.F. Approaches to outpatient pharmacy automation: A systematic review. *Eur. J. Hosp. Pharm.* **2019**, *26*, 157–162. [[CrossRef](#)]
14. Ahtiaainen, H.K.; Kallio, M.M.; Airaksinen, M.; Holmström, A.R. Safety, time and cost evaluation of automated and semi-automated drug distribution systems in hospitals: a systematic review. *Eur. J. Hosp. Pharm.* **2020**, *27*, 253–262. [[CrossRef](#)] [[PubMed](#)]
15. Zhu, S.; Wang, H.; Zhang, X.; He, X.; Tan, Z. A decision model on human-robot collaborative routing for automatic logistics. *Adv. Eng. Inform.* **2022**, *53*, 101681. [[CrossRef](#)]
16. Keung, K.; Lee, C.; Ji, P. Industrial internet of things-driven storage location assignment and order picking in a resource synchronization and sharing-based robotic mobile fulfillment system. *Adv. Eng. Inform.* **2022**, *52*, 101540. [[CrossRef](#)]
17. Boysen, N.; de Koster, R.; Füßler, D. The forgotten sons: Warehousing systems for brick-and-mortar retail chains. *Eur. J. Oper. Res.* **2020**, *288*, 361–381. [[CrossRef](#)]
18. Jin, H.; Yun, C.; Gao, X. Application and research of the refilling process with Clip Type Manipulator. In Proceedings of the 2015 IEEE International Conference on Robotics and Biomimetics (ROBIO), Zhuhai, China, 6–9 December 2015; pp. 775–780. [[CrossRef](#)]
19. Jin, H.; He, Q.; He, M.; Hu, F.; Lu, S. New method of path optimization for medical logistics robots. *J. Robot. Mechatronics* **2021**, *33*, 944–954. [[CrossRef](#)]
20. Yang, D.; Wu, Y.; Ma, W. Optimization of storage location assignment in automated warehouse. *Microprocess. Microsyst.* **2020**, *80*, 103356. [[CrossRef](#)]
21. Wu, L.; Huang, X.; Cui, J.; Liu, C.; Xiao, W. Modified adaptive ant colony optimization algorithm and its application for solving path planning of mobile robot. *Expert Syst. Appl.* **2023**, *215*, 1–22. [[CrossRef](#)]
22. Li, S.; Zhang, M.; Wang, N.; Cao, R.; Zhang, Z.; Ji, Y.; Li, H.; Wang, H. Intelligent scheduling method for multi-machine cooperative operation based on NSGA-III and improved ant colony algorithm. *Comput. Electron. Agric.* **2023**, *204*, 107532. [[CrossRef](#)]
23. Shi, E.; Lou, L.; Warburton, L.; Rubinsky, B. 3D Printing in Combined Cartesian and Curvilinear Coordinates. *J. Med. Devices* **2022**, *16*, 044502. [[CrossRef](#)]

24. Lanza, G.; Passacantando, M.; Scutellà, M.G. Assigning and sequencing storage locations under a two level storage policy: Optimization model and matheuristic approaches. *Omega* **2021**, *108*, 102565. [[CrossRef](#)]
25. Xu, X.; Ren, C. A novel storage location assignment in multi-pickers picker-to-parts systems integrating scattered storage, demand correlation, and routing adjustment. *Comput. Ind. Eng.* **2022**, *172*, 1–15. [[CrossRef](#)]
26. Ma, Z.; Wu, G.; Ji, B.; Wang, L.; Luo, Q.; Chen, X. A novel scattered storage policy considering commodity classification and correlation in robotic mobile fulfillment systems. *IEEE Trans. Autom. Sci. Eng.* **2022**, 1–14. [[CrossRef](#)]
27. Zuñiga, J.B.; Martínez, J.A.S.; Fierro, T.E.S.; Saucedo, J.A.M. Optimization of the storage location assignment and the picker-routing problem by using mathematical programming. *Appl. Sci.* **2020**, *10*, 534. [[CrossRef](#)]
28. Lu, F.; Feng, W.; Gao, M.; Bi, H.; Wang, S. The fourth-party logistics routing problem using ant colony system-improved grey wolf optimization. *J. Adv. Transp.* **2020**, *2020*, 8831746. [[CrossRef](#)]
29. Zhang, Z.; Xu, Z.; Luan, S.; Li, X.; Sun, Y. Opposition-Based Ant Colony Optimization Algorithm for the Traveling Salesman Problem. *Mathematics* **2020**, *8*, 1650. [[CrossRef](#)]
30. Jin, H.; Wang, W.; Cai, M.; Wang, G.; Yun, C. Ant colony optimization model with characterization-based speed and multi driver for the refilling system in hospital. *Adv. Mech. Eng.* **2017**, *9*, 1687814017713700. [[CrossRef](#)]

Disclaimer/Publisher’s Note: The statements, opinions and data contained in all publications are solely those of the individual author(s) and contributor(s) and not of MDPI and/or the editor(s). MDPI and/or the editor(s) disclaim responsibility for any injury to people or property resulting from any ideas, methods, instructions or products referred to in the content.